Supporting Material

Thrombin activity propagates in space during blood coagulation as an excitation wave

Authors: N.M. Dashkevich[*,†], M.V. Ovanesov[‡], A.N. Balandina[*,§], S.S. Karamzin[†], P.I. Shestakov[*,†], N.P. Soshitova[†], A.A. Tokarev[§], M.A. Panteleev[*,†,¶], F.I. Ataullakhanov[*,†,§,¶]

Affiliations:

[*] Center for Theoretical Problems of Physicochemical Pharmacology, Russian Academy of Sciences, 4 Kosygina St, Moscow, Russia, 119991

[†] HemaCore LLC, 3, 4th 8 Marta St, Moscow, Russia, 125319

[‡] Center for Biologics Evaluation and Research, U.S. Food and Drug Administration, 29 Lincoln Drive, N29/309, Bethesda, MD, USA, 20892

[§] Federal Research and Clinical Center of Pediatric Hematology, Oncology and Immunology, 1 Samory Mashela St, Moscow, Russia, 117198

[¶] Physics Department, Moscow State University, 1-2 Leninskie gory, Moscow, Russia, 119991, GSP-1

Corresponding author: Fazoil I Ataullakhanov, 3, 4th 8 Marta St, Moscow, Russia, 125319, tel +7 495 258 2538, e-mail: ataullakhanov.fazly@gmail.com

Table of contents

Data analysis

Algorithm overview.

The videomicroscopy system designed in this study monitored AMC (7-amino-4-methylcoumarin) cleavage from a fluorogenic substrate by thrombin during blood coagulation in the experimental chamber. Each experiment produced a series of images of i) light scattering intensity and ii) AMC fluorescence. These data were processed to calculate the spatial and temporal distributions of fibrin and thrombin in space and time, similarly to the strategy used in homogeneous thrombin generation assays (1). Images from red and UV light were processed similarly. To obtain light scattering or AMC fluorescence intensity profiles, the light intensity along the line perpendicular to the activator surface was measured for each frame. Values were averaged for 150–300 lines.

The clot growth rate was calculated from the movement of the point of half-maximal intensity of the light scattering profiles (2). The initial rate was calculated as the mean tangent of the size vs. time curve over the first 10 min of clot growth. The stationary rate was calculated similarly after 40 min of clot growth when the clot edge moved far enough away from the activator, such that its effect on clot growth became negligible.

To reconstruct the spatiotemporal distribution of proteolytic enzyme activity, the reaction-diffusion equation was used:

$$\frac{\partial[AMC]}{\partial t} = D_{AMC} \cdot \frac{\partial^2[AMC]}{\partial x^2} + \frac{k_{cat} \cdot [S] \cdot [IIa]}{K_M + [S]}, \qquad \text{(S1)}$$

where $[AMC]$ is the AMC concentration; D_{AMC} is the AMC diffusion coefficient; k_{cat} and K_M are the catalytic and Michaelis constants of substrate cleavage, respectively; $[IIa]$ is the thrombin concentration; and $[S]$ is the substrate concentration. This equation can be used to derive the thrombin concentration:

$$[IIa] = \frac{K_M + [S]}{k_{cat} \cdot [S]} \cdot \left(\frac{\partial[AMC]}{\partial t} - D_{AMC} \cdot \frac{\partial^2[AMC]}{\partial x^2} \right), \qquad \text{(S2)}$$

Numerical differentiation of an experimentally obtained signal is an “incorrectly posed problem”, in which large noises in the final outcome can easily occur from slight noises in the

initial signal. In addition, the procedure of thrombin reconstruction can be subject to numerous disturbances, such as nonuniformity of illumination, AMC bleaching, fluorescence distortion by fibrin clot, or binding of AMC in plasma, leading to altered diffusion velocity. Therefore, additional steps were included in the algorithm, as detailed below. Parameters for the algorithm are given in Table S1.

Calculating AMC concentration from fluorescence.

The AMC intensity profiles were transformed into concentration profiles by calibration. The calibration intensity profile I_{cal} was calculated on the basis of an image of uniform distribution of known AMC concentration in the same plasma. The AMC concentration at each point [AMC_i] was calculated from the fluorescence intensity I_i by using the background fluorescence profile I_{bgr} and AMC concentration in the calibration sample [AMC_{cal}]:

$$[AMC_i] = \frac{(I_i - I_{bgr}) * [AMC_{cal}]}{(I_{cal} - I_{bgr})} \quad \text{(S3)}$$

Correction of fibrin-clot-induced distortion.

The fluorescence intensity was increased in the presence of fibrin clot. This increase was proportional to both fibrin and AMC concentrations. (Fig. S1) To correct for fluorescence distortion, the following equation was used:

$$[AMC_{app}] = [AMC] + (k_1 + k_2 \cdot [AMC]) \cdot \frac{F}{k_3}, \quad \text{(S4)}$$

where $[AMC_{app}]$ is the apparent AMC concentration obtained from the previous procedure, $[AMC]$ is the true AMC concentration, F is the fibrin light scattering intensity, and k_1-k_3 are the experimental setup-dependent parameters.

Effect of AMC binding in plasma on the diffusion velocity.

Experiments to assess AMC binding in plasma revealed that there are binding sites for AMC provided (most likely) by serum albumin, and that a significant quantity of AMC is always in a bound state. (Fig. S2) Therefore, the effective diffusion of AMC was reduced. This finding led to a correction of the initial Eq. 1:

$$\frac{\partial[AMC]}{\partial t} = D_{AMC} \cdot \frac{\partial^2[AMC^{free}]}{\partial x^2} + D_{BSA} \cdot \frac{\partial^2[AMC^{BSA}]}{\partial x^2} + \frac{k_{cat} \cdot [S] \cdot [IIa]}{K_M + [S]}, \quad \text{(S5)}$$

$$[AMC^{bound}] = [AMC] - [AMC^{free}] = 0.67 \cdot [AMC], \quad \text{(S6)}$$

Effect of fibrin clot on thrombin: a control.

To investigate if clot formation regulates thrombin generation via reversible inhibition of thrombin by fibrin, or via protection of thrombin from inhibition by antithrombin III, or via acceleration of factor XI activation, we depleted fibrinogen using a fibrin-cleaving protease from snake venom. In defibrinated plasma, thrombin spatial propagation was qualitatively similar (Fig. S3) indicating that thrombin wave propagation is not determined by formation of polymerized fibrin clot.

Selection of a numerical method for calculation of the derivatives.

To summarize, the set of equations required to obtain thrombin from the AMC distribution were of the form:

$$\begin{cases} [IIa] = \dfrac{K_M + [S]}{k_{cat} \cdot [S]} \cdot \left(\dfrac{\partial[AMC]}{\partial t} - D_{AMC} \cdot \dfrac{\partial^2[AMC^{free}]}{\partial x^2} - D_{BSA} \cdot \dfrac{\partial^2[AMC^{BSA}]}{\partial x^2} \right) \\ [AMC^{bound}] = [AMC] - [AMC^{free}] = 0.67 \cdot [AMC] \\ \dfrac{\partial[S]}{\partial t} = D_S \cdot \dfrac{\partial^2[S]}{\partial x^2} - \dfrac{k_{cat} \cdot [S] \cdot [IIa]}{K_M + [S]} \\ S\big|_{t=0} = S_0 \end{cases} \quad \text{(S7)}$$

The contribution of substrate diffusion was extremely small and was usually neglected. To reduce noise, the following algorithm was used to calculate derivatives:

$$\frac{\partial[AMC]}{\partial t} = \frac{[AMC]_{x,t+j\cdot\Delta t} - [AMC]_{x,t}}{j \cdot \Delta t} \quad \text{(S8)}$$

$$\frac{\partial^2[AMC]}{\partial x^2} = \frac{[AMC]_{x+i\cdot\Delta x,t} - 2\cdot[AMC]_{x,t} + [AMC]_{x-i\cdot\Delta x,t}}{(i \cdot \Delta x)^2} \quad \text{(S9)}$$

where Δt is the time between frames (usually 1 min) and Δx is pixel size (usually 4.3 microns). The parameter values $i = 60$ and $j = 3$ were chosen to be optimal for maximal noise reduction and minimal signal distortion.

This algorithm was able to reconstruct thrombin activity distribution in space and time (Figure 1). However, the regions very close to the activator (200–300 μm) were not reconstructed, and the contribution of the α_2-macroglobulin complex with thrombin to AMC production (3) was neglected.

Computer simulations

Model design.

Blood coagulation was simulated as a 1D process on a (0, L) interval, with L = 4 mm and tissue factor (TF) located at $x = 0$. The model included 24 partial differential equations for reactants in plasma and two ordinary differential equations for the density of the TF-containing complexes on the activator. The model was numerically integrated by using the embedded Runge-Kutta-Fehlberg method of the order 2(3) as described (4).

Notation.

The following notation is used throughout this paper. Concentration designations are as follows: x_j, concentration of the j^{th} active coagulation factor; y_j, concentration of the inactive precursor of the j^{th} coagulation factor; i_j, concentration of the j^{th} inhibitor; $x_{i\text{-}j}$, concentration of the complex of the i^{th} and j^{th} factors; x_j^F, concentration of the free j^{th} factor (not bound to another factor or phospholipid membrane); x_j^{BF}, concentration of the free j^{th} factor on the membrane (not in complex with another factor on the same membrane); and x_j^S, surface densities of TF, factor VII, factor VIIa, and their complexes. All initial concentrations are summarized in Table S2.

Parameter designations are as follows: k_j, kinetic constant or forward rate constant of the j^{th} reaction; k_{-j}, backward rate constant of the j^{th} reaction; K_j, the Michaelis or equilibrium constant of the j^{th} reaction; n_j, number of membrane binding sites for the j^{th} factor; and h_j, rate constant of the j^{th} inhibition reaction. All constants are summarized in Table S3.

Dimensions are as follows: distance [x] = mm, time [t] = min, volume concentrations [x_j, y_j, etc.] = nM, and surface densities [x_3, x_7, y_7, $x_{7\text{-}3}$, $y_{7\text{-}3}$] = nmol/mm^2.

Model description.

The quantitative mechanism-driven mathematical model was based on a model published recently by the authors (5). The model was modified to take into account the use of another activator, the transition to a reaction-diffusion system (6), and introduction of a fluorogenic substrate and phospholipids. The most important modifications were as follows: 1) all variables were separated into those described by partial and ordinary equations as described above; 2) interactions of thrombin and thrombomodulin were added; 3) interactions of thrombin and factor Xa with Z-Gly-Gly-Arg-AMC were added; 4) all diffusion coefficients (6) were corrected for plasma viscosity and temperature by multiplying by 0.88; 5) only free factors (not bound to membranes) were allowed to diffuse; and 6) to account for the effects of the phospholipid membrane, the multiplicator of $p/(1+p/K_p)$ was substituted for p in all equations.

Variable pools.

All equations are for total concentrations of coagulations factors. For example, factor Xa is presumably distributed between free factor, prothrombinase complex, substrate-bound, etc:

$$x_{10} = x_{10}^{\ F} + x_{10-5}^{\ B} + x_{10}^{S} + x_{10-5}^{S\ B} \tag{S10}$$

To calculate the thrombin activity observed in the experiment, the following equation was used:

$$x_{2,\exp} = x_2^{S} + x_2^{\ F} + \frac{x_{2-M}}{2}, \tag{S11}$$

which accounts for the fact that α_2-macroglobulin-bound thrombin has ~50% of free thrombin activity towards Z-Gly-Gly-Arg-AMC.

Model equations.

$$\text{TF}^{\text{S}}\text{:}\ \frac{dx_3^{\ S}}{dt} = -\left(k_1 \cdot x_7 \cdot x_3^{\ S} - k_{-1} \cdot x_{7-3}^{\ S\ F}\right) - \left(k_1 \cdot y_7 \cdot x_3^{\ S} - k_{-1} \cdot y_{7-3}^{\ S}\right) \tag{S12}$$

$$\text{VII–TF}^{\text{S}}\text{:}\ \frac{dy_{7-3}^{\ S}}{dt} = \left(k_1 \cdot y_7 \cdot x_3^{\ S} - k_{-1} \cdot y_{7-3}^{\ S}\right) - \left(k_2 \cdot x_2^{\ F} + k_3 \cdot x_{10}^{\ F}\right) \cdot y_{7-3}^{\ S} \tag{S13}$$

VIIa–TF^S: $\frac{dx_{7-3}{}^{S}}{dt} = \left(k_1 \cdot x_7 \cdot x_3{}^{S} - k_{-1} \cdot x_{7-3}{}^{SF}\right) + \left(k_2 \cdot x_2{}^{F} + k_3 \cdot x_{10}{}^{F}\right) \cdot y_{7-3}{}^{S} - h_1 \cdot x_{7-3}{}^{SF} \cdot i_3 - h_2 \cdot x_{10-7-3}{}^{S} \cdot i_2$ (S14)

VII: $-D_{VII} \cdot \frac{\partial y_7}{\partial x} = -\left(k_1 \cdot y_7 \cdot x_3{}^{S} - k_{-1} \cdot y_{7-3}{}^{S}\right)$ (S15)

VIIa: $-D_{VIIa} \cdot \frac{\partial x_7}{\partial x} = -\left(k_1 \cdot x_7 \cdot x_3{}^{S} - k_{-1} \cdot x_{7-3}{}^{SF}\right)$ (S16)

IX: $-D_{IX} \cdot \frac{\partial y_9}{\partial x} = -\mathrm{F_{IX}}$, where $\mathrm{F_{IX}} = \frac{k_4}{K_4} \cdot y_9 \cdot x_{7-3}{}^{SF}$ (S17)

IXa: $-D_{IXa} \cdot \frac{\partial x_9}{\partial x} = \frac{\mathrm{F_{IX}}}{1 - \frac{n_{20}}{K_{20} + x_9} \cdot \frac{p}{1 + \frac{p}{K_p}} \cdot \left(1 - \frac{x_9}{K_{20} + x_9}\right)}$ (S18)

X: $-D_X \cdot \frac{\partial y_{10}}{\partial x} = -\mathrm{F_X}$, where $\mathrm{F_X} = \frac{k_6}{K_6} \cdot y_{10} \cdot x_{7-3}{}^{SF}$ (S19)

Xa: $-D_{Xa} \cdot \frac{\partial x_{10}}{\partial x} = \frac{F_X \cdot \left(1 + \frac{S}{K_{S,10}}\right)}{1 - \frac{x_5{}^{B}}{K_{23} \cdot \left(1 + \frac{i_{12}}{K_{24}}\right) + x_{10} + x_5{}^{B}} \cdot \frac{1}{1 + \frac{p}{K_p}} \cdot \left(1 - \frac{x_{10}}{K_{23} \cdot \left(1 + \frac{i_{12}}{K_{24}}\right) + x_{10} + x_5{}^{B}}\right)}$ (S20)

TFPI: $-D_{TFPI} \cdot \frac{\partial i_2}{\partial x} = -h_2 \cdot x_{10-7-3}{}^{SF} \cdot i_2$ (S21)

Xa-TFPI complex: $-D_{Xa-TFPI} \cdot \frac{\partial i_3}{\partial x} = -h_1 \cdot x_{7-3}{}^{SF} \cdot i_3$ (S22)

VII: $\frac{\partial y_7}{\partial t} = D_{VII} \cdot \frac{\partial^2 y_7}{\partial x^2} - k_2 \cdot y_7 \cdot x_2{}^{F}$ (S23)

VIIa: $\frac{\partial x_7}{\partial t} = D_{VIIa} \cdot \frac{\partial^2 x_7}{\partial x^2} + k_2 \cdot y_7 \cdot x_2{}^{F}$ (S24)

IX: $\frac{\partial y_9}{\partial t} = D_{IX} \cdot \frac{\partial^2 y_9}{\partial x^2} - \mathrm{R_{IX}}$, where $\mathrm{R_{IX}} = \frac{k_5 \cdot y_9 \cdot x_{11}}{K_5 + y_9}$ (S25)

IXa: $\frac{\partial x_9}{\partial t} = D_{IXa} \cdot \frac{\partial^2}{\partial x^2}\left(x_9 - x_9^{B^F}\right) + \mathrm{R_{IX}} - h_3 \cdot i_1 \cdot x_9$ (S26)

X: $\frac{\partial y_{10}}{\partial t} = D_X \cdot \frac{\partial^2}{\partial x^2}\left(y_{10} - y_{10}^B\right) - \mathrm{R_X}$, where $\mathrm{R_X} = \frac{k_7 \cdot x_9^{B^F} \cdot y_{10}^B}{p \cdot K_7} +$

$+ \frac{k_8 \cdot x_9^{B^F} \cdot x_8^{B^F} \cdot y_{10}^B}{p^2 \cdot K_9 \cdot K_8}$ (S27)

Xa: $\frac{\partial x_{10}}{\partial t} = D_{Xa} \cdot \frac{\partial^2}{\partial x^2}\left(x_{10}^F \cdot \left(1 + \frac{S}{K_{S,10}}\right)\right) + \mathrm{R_X} - \left(k_{11} \cdot x_{10}^F \cdot i_2 - k_{-11} \cdot i_3\right) -$

$-\left(h_4 \cdot i_1 + h_5 \cdot i_6 + h_6 \cdot i_7 + h_7 \cdot i_{10}\right) \cdot x_{10}^F - h_8 \cdot i_1 \cdot x_{10-5}^B$ (S28)

II: $\frac{\partial y_2}{\partial t} = D_{II} \cdot \frac{\partial^2}{\partial x^2}\left(y_2 - y_2^B\right) - \mathrm{R_{II}}$,

where $\mathrm{R_{II}} = k_{12} \cdot \frac{x_{10}^F \cdot p}{\left(1 + \frac{p}{K_p}\right)^2} \cdot y_2 + k_{13} \cdot \frac{x_{10-5}^B}{p \cdot \left(1 + \frac{S}{K_{S,10}}\right)} \cdot y_2^B$ (S29)

IIa: $\frac{\partial x_2}{\partial t} = D_{IIa} \cdot \frac{\partial^2}{\partial x^2}\left(x_2^F + x_2^S\right) + D_{Fg} \cdot \frac{\partial^2}{\partial x^2} x_2^{Fg} + D_{Fn} \cdot \frac{\partial^2}{\partial x^2} x_2^{Fn} + \mathrm{R_{II}} -$

$-\left(h_9 \cdot i_1 + h_{11} \cdot i_7 + h_{12} \cdot i_{10} + h_{13} \cdot i_9\right) \cdot x_2^F - \mathrm{R_{IIa\text{-}M}} - \left(k_{28} \cdot i_{13} \cdot x_2^F - k_{-28} \cdot x_{2-Tm}\right)$ (S30)

IIa-α_2M: $\frac{\partial x_{2-M}}{\partial t} = D_{\alpha_2 M} \cdot \frac{\partial^2 x_{2-M}}{\partial x^2} + \mathrm{R_{IIa\text{-}M}}$, where $\mathrm{R_{IIa\text{-}M}} = h_{10} \cdot i_6 \cdot \left(x_2^F + x_2^S\right)$ (S31)

IIa-Tm: $\frac{\partial x_{2-Tm}}{\partial t} = D_{IIa-Tm} \cdot \frac{\partial^2 x_{2-Tm}}{\partial x^2} + \left(k_{28} \cdot i_{13} \cdot x_2^F - k_{-28} \cdot x_{2-Tm}\right) -$

$-\left(h_{25} \cdot i_1 + h_{26} \cdot i_{10}\right) \cdot x_{2-Tm}$ (S32)

Fibrin: $\frac{\partial x_1}{\partial t} = D_{Fn} \cdot \frac{\partial^2 x_1}{\partial x^2} + \mathrm{R_{Fn}}$, where $\mathrm{R_{Fn}} = \frac{k_{14}}{K_{14}} \cdot y_1 \cdot x_2^F$ (S33)

Fibrinogen: $\frac{\partial y_1}{\partial t} = D_{Fg} \cdot \frac{\partial^2 y_1}{\partial x^2} - \mathrm{R_{Fn}}$ (S34)

VIII: $\frac{\partial y_8}{\partial t} = D_{VIII} \cdot \frac{\partial^2 y_8}{\partial x^2} - \mathrm{R_{VIII}}$, where $\mathrm{R_{VIII}} = \frac{k_{15} \cdot y_8 \cdot x_2^F}{K_{15} + x_2^F}$ (S35)

VIIIa: $\frac{\partial x_8}{\partial t} = D_{VIIIa} \cdot \frac{\partial^2}{\partial x^2}\left(x_8 - x_8^{B^F}\right) + \mathrm{R_{VIII}} - h_{14} \cdot x_8$ (S36)

V: $\frac{\partial y_5}{\partial t} = D_V \cdot \frac{\partial^2 y_5}{\partial x^2} - \mathrm{R_V}$, where $\mathrm{R_V} = \frac{k_{16} \cdot y_5 \cdot {x_2}^F}{K_{16} + {x_2}^F}$ (S37)

Va: $\frac{\partial x_5}{\partial t} = D_{Va} \cdot \frac{\partial^2}{\partial x^2}\left(x_5 - {x_5}^B\right) + \mathrm{R_V} - h_{15} \cdot i_4 \cdot {x_5}^{BF}$ (S38)

XI: $\frac{\partial y_{11}}{\partial t} = D_{XI} \cdot \frac{\partial^2 y_{11}}{\partial x^2} - \mathrm{R_{XI}}$, where $\mathrm{R_{XI}} = k_{17} \cdot y_{11} \cdot {x_2}^F \cdot \frac{p}{1 + \frac{p}{K_p}}$ (S39)

XIa: $\frac{\partial x_{11}}{\partial t} = D_{XIa} \cdot \frac{\partial^2 x_{11}}{\partial x^2} + \mathrm{R_{XI}} - \left(h_{16} \cdot i_1 + h_{17} \cdot i_8 + h_{18} \cdot i_7 + h_{19} \cdot i_{10} + h_{20} \cdot i_{11}\right) \cdot x_{11}$ (S40)

AT-III: $\frac{\partial i_1}{\partial t} = D_{ATIII} \cdot \frac{\partial^2 i_1}{\partial x^2} - \left(h_3 \cdot x_9 + h_4 \cdot {x_{10}}^F + h_8 \cdot {x_{10-5}}^B + h_9 \cdot {x_2}^F + h_{16} \cdot x_{11}\right) \cdot i_1 -$

$- h_{25} \cdot i_1 \cdot x_{2-Tm}$ (S41)

TFPI: $\frac{\partial i_2}{\partial t} = D_{TFPI} \cdot \frac{\partial^2 i_2}{\partial x^2} - \left(k_{11} \cdot {x_{10}}^F \cdot i_2 - k_{-11} \cdot i_3\right) - h_2 \cdot {x_{10-7-3}}^V \cdot i_2$ (S42)

Xa–TFPI: $\frac{\partial i_3}{\partial t} = D_{Xa-TFPI} \cdot \frac{\partial^2 i_3}{\partial x^2} + \left(k_{11} \cdot {x_{10}}^F \cdot i_2 - k_{-11} \cdot i_3\right) - h_1 \cdot {x_{7-3}}^{VF} \cdot i_3$ (S43)

PC: $\frac{\partial i_5}{\partial t} = D_{PC} \cdot \frac{\partial^2 i_5}{\partial x^2} - \mathrm{R_{PC}}$, where $\mathrm{R_{PC}} = k_{18} \cdot i_5 \cdot {x_2}^F + \frac{k_{29} \cdot i_5 \cdot x_{2-Tm}}{K_{29} + i_5}$ (S44)

APC: $\frac{\partial i_4}{\partial t} = D_{PCa} \cdot \frac{\partial^2 i_4}{\partial x^2} + \mathrm{R_{PC}} - \left(h_{21} \cdot i_6 + h_{22} \cdot i_8 + h_{23} \cdot i_7 + h_{24} \cdot i_{10}\right) \cdot i_4$ (S45)

Tm: $\frac{\partial i_{13}}{\partial t} = D_{Tm} \cdot \frac{\partial^2 i_{13}}{\partial x^2} - \left(k_{28} \cdot i_{13} \cdot {x_2}^F - k_{-28} \cdot x_{2-Tm}\right) + \left(h_{25} \cdot i_1 + h_{26} \cdot i_{10}\right) \cdot x_{2-Tm}$ (S46)

Free VIIa–TF: ${x_{7-3}}^{SF} = \frac{{x_{7-3}}^S}{1 + \frac{y_9}{K_4} + \frac{y_{10}}{K_6}}$ (S47)

Xa–VIIa–TF: ${x_{10-7-3}}^S = \frac{k_6}{K_6 \cdot k_{-19}} \cdot y_{10} \cdot {x_{7-3}}^{SF}$ (S48)

Free lipid-bound IXa: ${x_9}^{BF} = \frac{x_9 \cdot n_{20}}{K_{20} + x_9} \cdot \frac{p}{1 + \frac{p}{K_p}}$ (S49)

Free lipid-bound VIIIa: $x_8^{BF} = \frac{x_8 \cdot n_{21}}{(K_{21} + x_8) \cdot \left(1 + \frac{y_{10}^{B}}{p \cdot K_{10}}\right) \cdot \left(1 + \frac{i_{12}}{K_{22}}\right)} \cdot \frac{p}{1 + \frac{p}{K_p}}$ (S50)

Lipid-bound Xa–Va: $x_{10\text{–}5}^{B} = \frac{x_{10} \cdot x_5^{B}}{K_{23} \cdot \left(1 + \frac{i_{12}}{K_{24}} + \frac{x_{10}}{K_{23}}\right) + x_5^{B}} \cdot \frac{1}{1 + \frac{p}{K_p}} \cdot \frac{1}{1 + \frac{S}{K_{S,10}}}$ (S51)

Free Xa: $x_{10}^{F} = \frac{x_{10}}{1 + \frac{S}{K_{S,10}}} - x_{10\text{–}5}^{B}$ (S52)

Xa– Z-Gly-Gly-Arg-AMC complex: $x_{10}^{S} = x_{10}^{F} \cdot \frac{S}{K_{S,10}}$

(S53)

Lipid-bound Va–Xa– Z-Gly-Gly-Arg-AMC: $x_{10\text{–}5}^{S\ B} = x_{10\text{–}5}^{B} \cdot \frac{S}{K_{S,10}}$ (S54)

Lipid-bound X: $y_{10}^{B} = \frac{y_{10} \cdot n_{25}}{K_{25} \cdot \left(1 + \frac{y_{10}}{K_{25}} + \frac{y_2}{K_{26}}\right)} \cdot \frac{p}{1 + \frac{p}{K_p}}$ (S55)

Free thrombin: $x_2^{F} = \frac{x_2}{1 + \frac{x_1 + y_1}{K_{14}} + \frac{S}{K_{S,2}}}$ (S56)

IIa– Z-Gly-Gly-Arg-AMC: $x_2^{S} = x_2^{F} \cdot \frac{S}{K_{S,2}}$ (S57)

Thrombin–fibrinigen complex: $x_2^{Fg} = x_2^{F} \cdot \frac{y_1}{K_{14}}$ (S58)

Thrombin–fibrin complex: $x_2^{Fn} = x_2^{F} \cdot \frac{x_1}{K_{14}}$ (S59)

Lipid-bound prothrombin: $y_2^{B} = \frac{y_2 \cdot n_{25}}{K_{26} \cdot \left(1 + \frac{y_{10}}{K_{25}} + \frac{y_2}{K_{26}}\right)} \cdot \frac{p}{1 + \frac{p}{K_p}}$ (S60)

Lipid-bound Va: $x_5^{B} = \frac{x_5 \cdot p \cdot n_{27}}{K_{27} + x_5}$ (S61)

Lipid-bound free Va: $x_5{}^{BF} = x_5{}^{B} - x_{10-5}{}^{B}$ (S62)

Supporting Figures

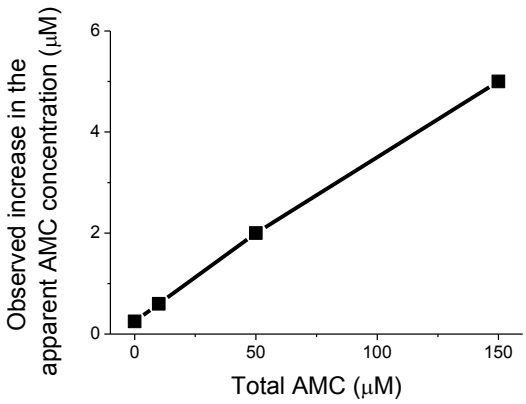

Fig. S1. Effect of fibrin clot on AMC fluorescence. Clot formation was initiated in recalcified plasma by a high-density TF activator in the presence of different AMC concentrations or in the absence of any fluorogenic substrate. A typical linear (R = 0.9993) "apparent" increase of AMC concentration caused by fibrin clot formation is shown.

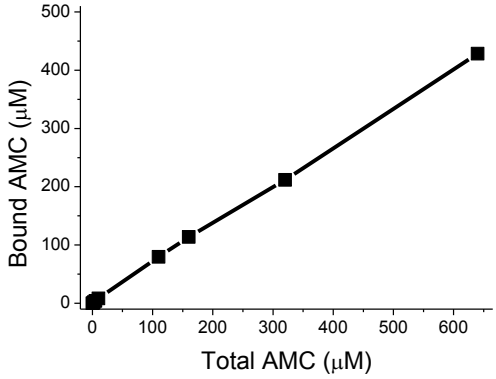

Fig. S2. AMC binding in plasma. Different concentrations of AMC were added to pooled normal plasma (n = 3) incubated in a plastic cup with stirring. A PBS-filled dialysis unit with a separation threshold of 3500 kDa was inserted into the plasma. The AMC was allowed to equilibrate between the plasma and buffer. The AMC concentration in PBS was calculated on the basis of the fluorescence (λ_{ex} 355 nm, λ_{em} 460 nm) by using the calibration curve. The bound AMC concentration was determined by subtracting the free AMC concentration from the total concentration. A linear fitting revealed that 67% ± 1% of the AMC was bound (R = 0.9995). The value was stable (±5%) across different plasmas. Similar results were obtained when a solution of BSA (50 mg/mL) was used instead of plasma.

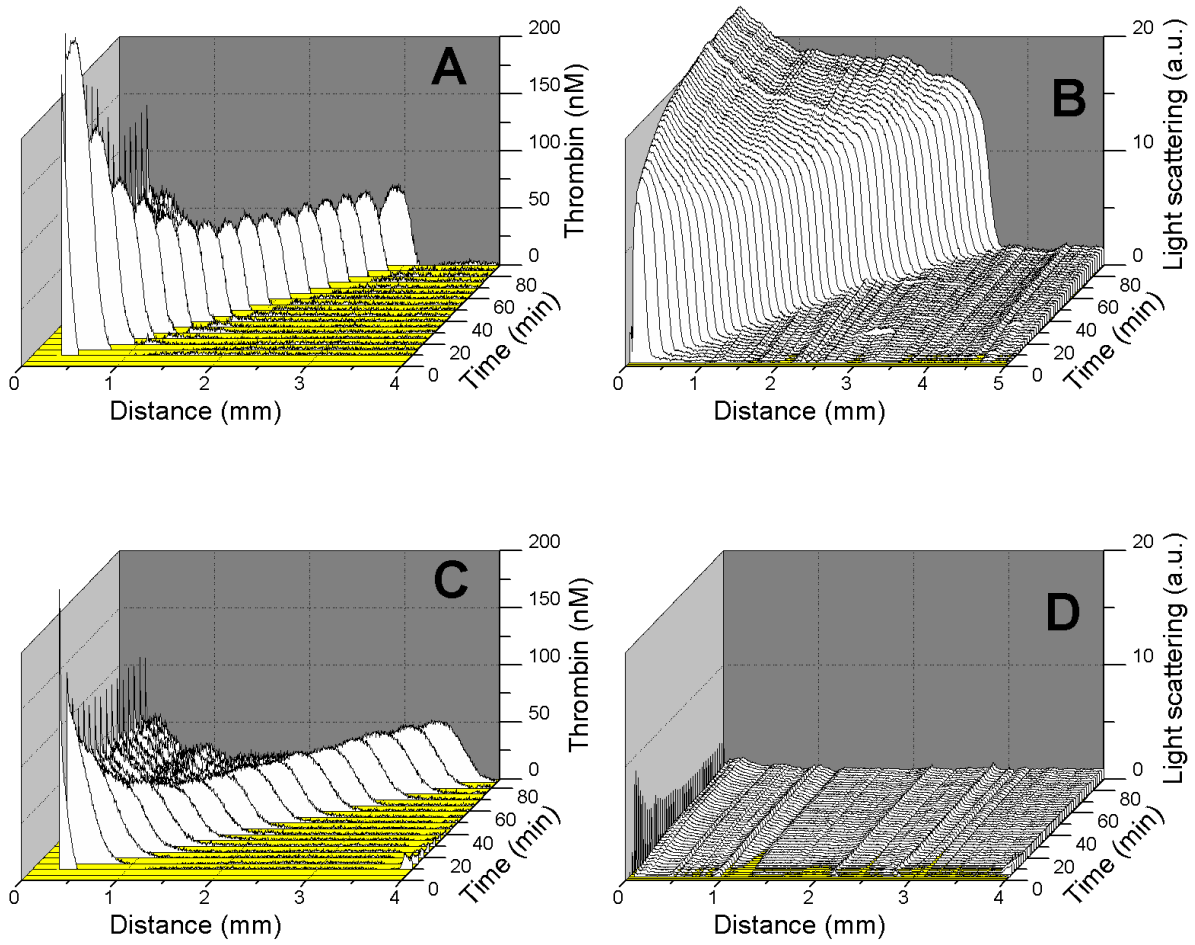

Fig. S3. Spatial thrombin propagation in defibrinated plasma. Panels display thrombin **(A, C)** or fibrin **(B, D)** distribution in time and space after stimulation of clotting in normal plasma: control plasma **(A, B)** or plasma defibrinated with ancistron **(C, D)**. Activation was caused by TF at 90 pmol/m^2. Experiments were performed in 0.5% agarose gel in the presence of 10 μM phospholipids.

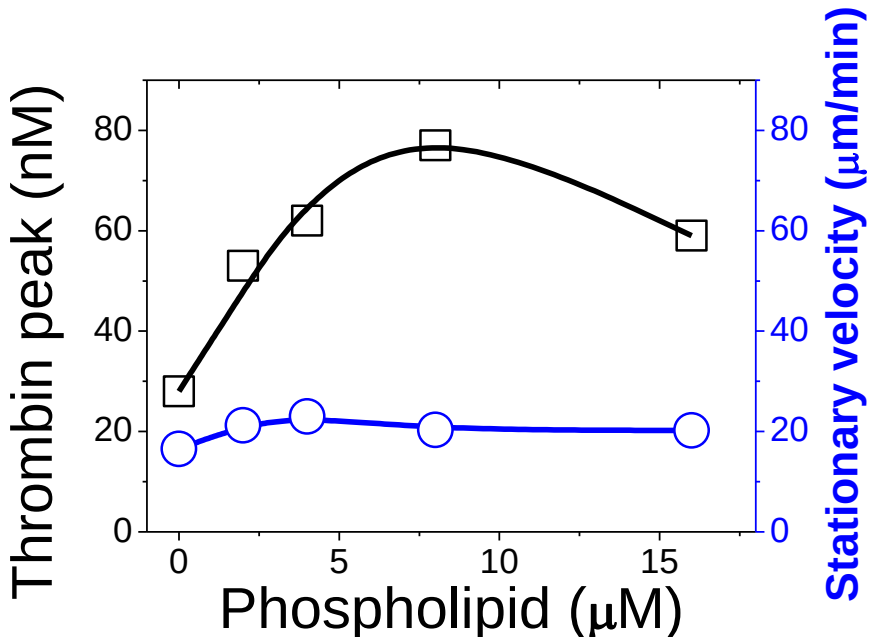

Fig. S4. Regulation of spatial thrombin propagation by phospholipids. Thrombin peak height **(black squares)** and spatial velocity **(blue circles)** of fibrin clot propagation as functions of phospholipid concentration in a typical experiment (out of n = 6) in normal plasma. Stimulation is with TF at 90 pmol/m^2.

.

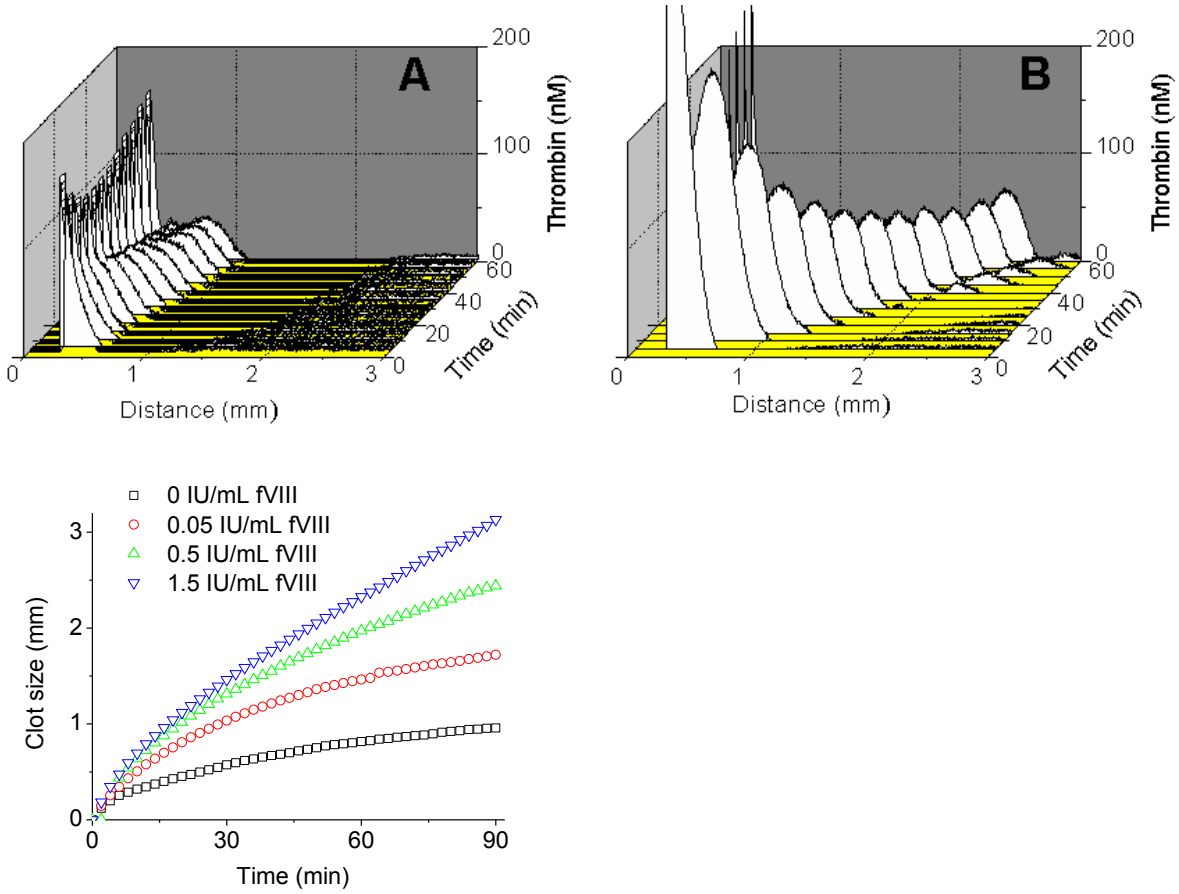

Fig. S5. Spatial thrombin propagation in factor VIII-deficient plasma. (**A**) and (**B**) Thrombin distribution in time and space after clot stimulation in factor VIII-deficient plasma supplemented with or without 1.5 IU/mL of factor VIII. (***C***) Clot size as a function of time for different factor VIII (fVIII) concentrations. A typical series of experiments is shown (out of n = 2).

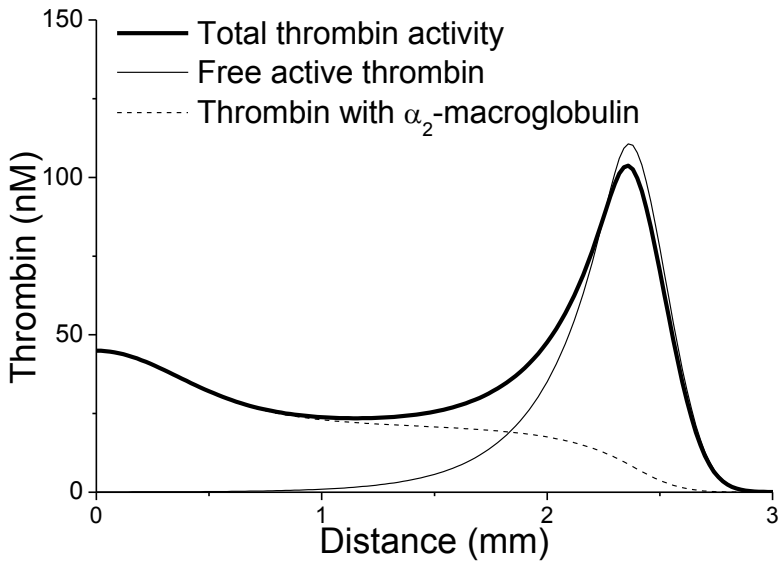

Fig. S6. Shape of the thrombin wave in the mathematical model. Spatial distribution of thrombin activity in normal plasma with regard to the Z-GGR-AMC measured experimentally ($x_{2,\mathrm{exp}}$), free active thrombin with regard to coagulation proteins (x_2), and the activity of the thrombin–α_2-macroglobulin complex after 50 min of simulation. The results are similar to the experimental findings obtained in this study. Note that a significant portion of thrombin activity near the activator is not thrombin, but the thrombin–α_2-macroglobulin complex.

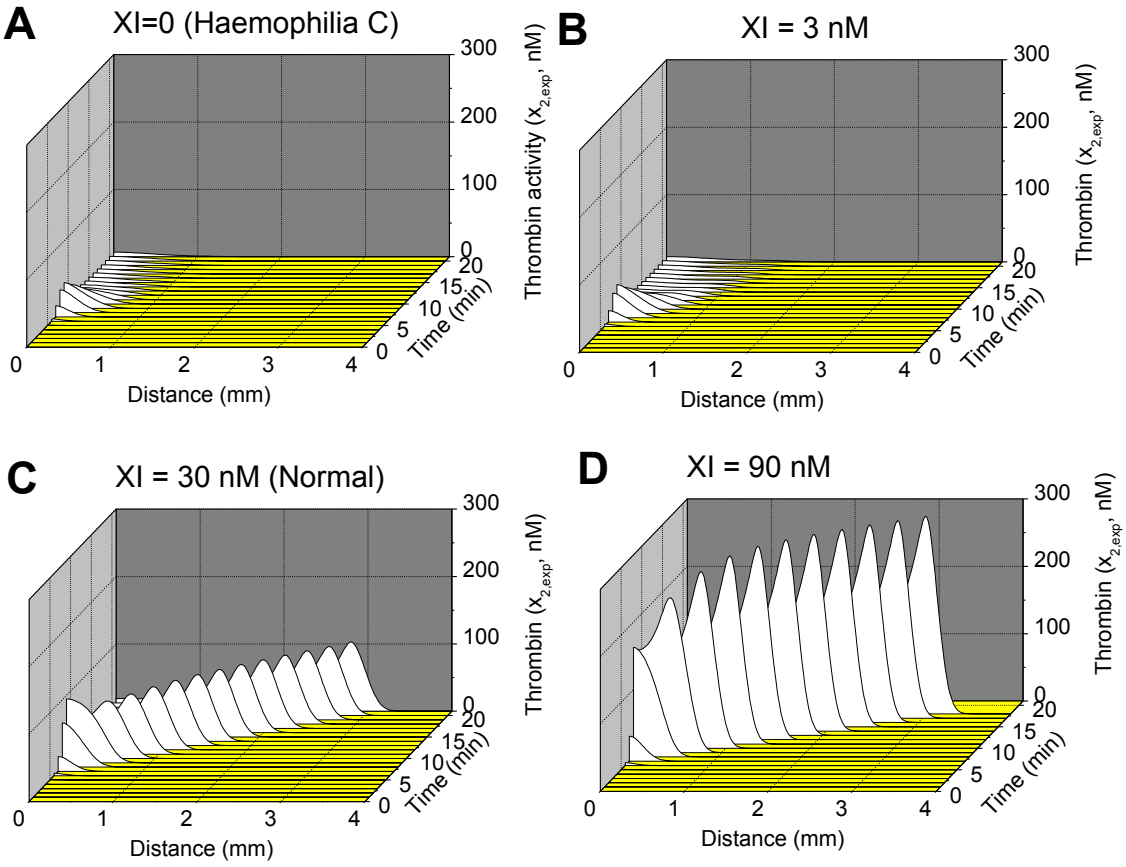

Fig. S7. Thrombin wave propagation at different factor XI concentrations in the mathematical model. Factor XI is necessary for formation of the traveling thrombin wave in the mathematical model, which is consistent with the experiments shown in Figure 3. Thus, the experimental findings of the study are consistent with current theoretical knowledge of how the coagulation system is regulated.

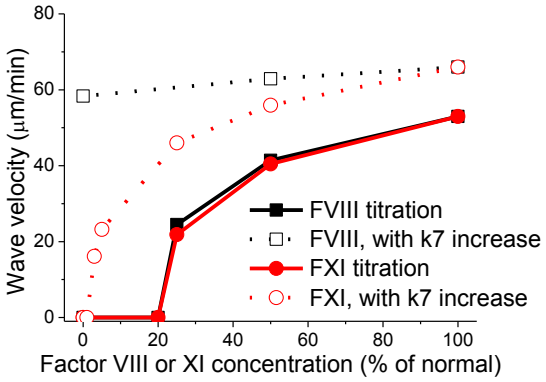

Fig. S8. Distinct roles of factor XI and factor VIII activation. Computer simulations of the velocity of the traveling wave of thrombin, as a function of the coagulation factor concentration, with or without 1000-fold free factor IXa efficiency increase obtained from computer simulations. Factor XI-dependent feedback is principally indispensable for the formation of the traveling wave. In other words, both factors are needed for a wave to appear. An artificial 1000-fold increase in the catalytic efficiency of free factor IXa (not bound to the intrinsic tenase complex with factor VIIIa) can stimulate wave formation even without factor VIII. Factor XI is indispensable because without it, no increase of these rate constants will produce a traveling wave.

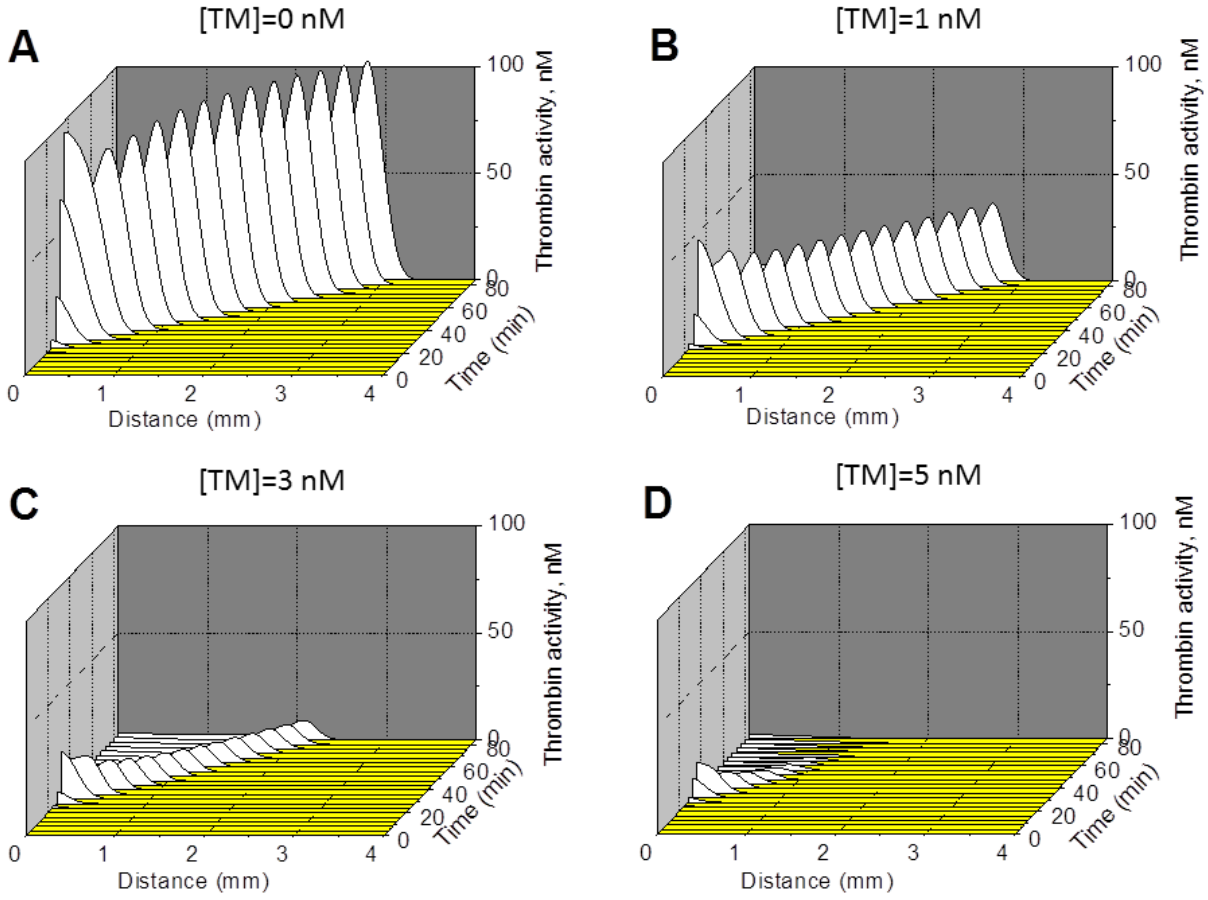

Fig. S9. Effect of soluble thrombomodulin on thrombin propagation in the mathematical model. Computer simulation of thrombin propagation in presence of increasing concentrations of soluble thrombomudulin that is in consistent with the experiment shown in Figure 4. [TF]=0.05 pmol/m^2

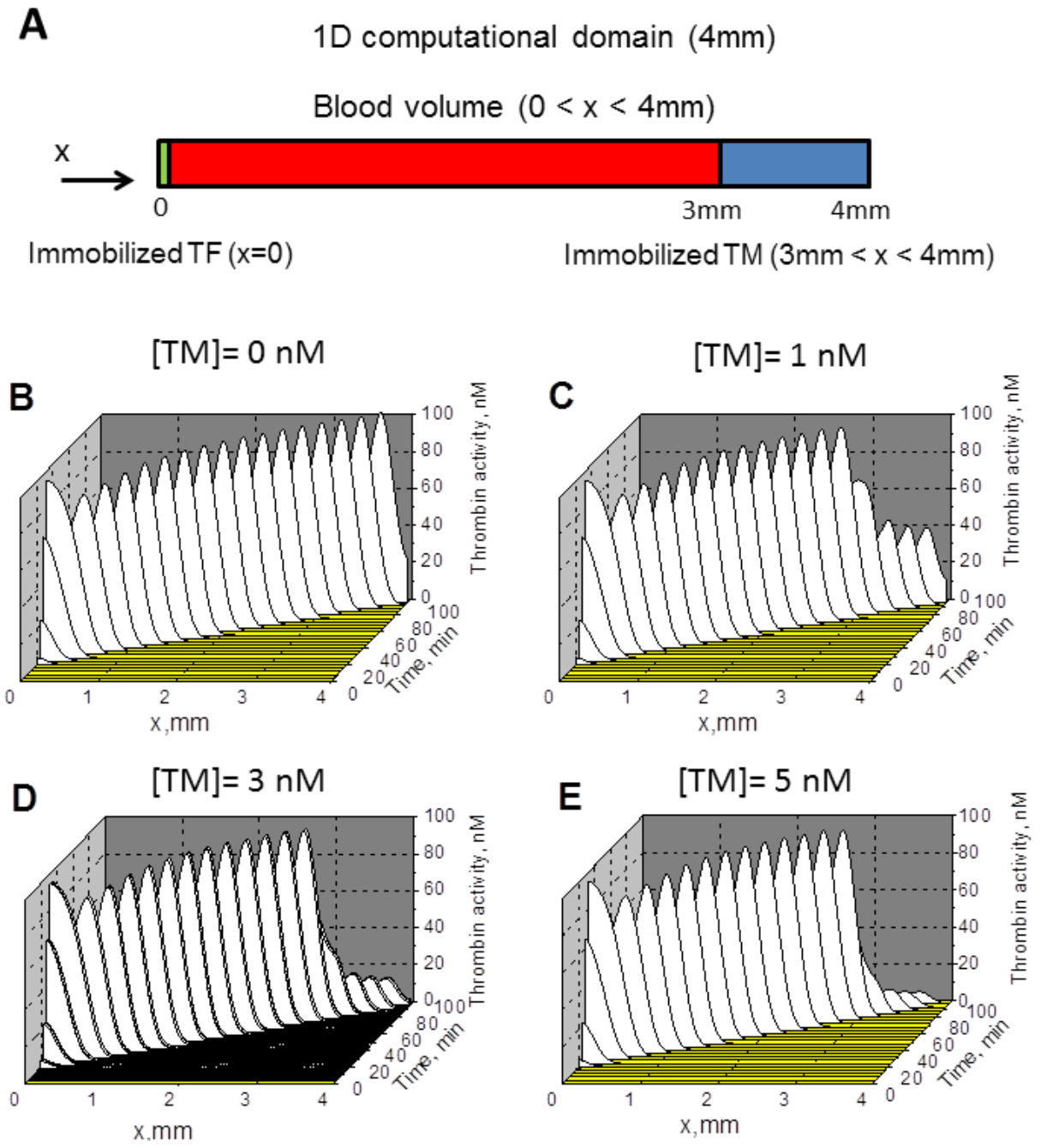

Fig S10. Immobilized thrombomodulin stops thrombin wave propagation in the mathematical model. When TM is localized far from the activating surface (*A*) it still has effect on thrombin distribution. TM decreases thrombin peak height and thereby stops thrombin propagation.

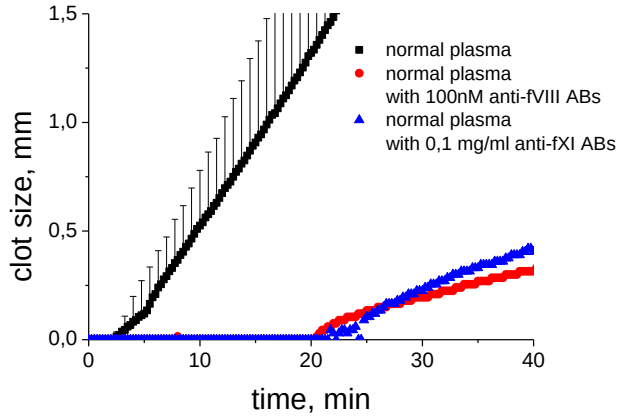

Fig. S11. Effect of anti-fVIII and anti-fXI antibodies on clot growth. Clot size vs time plots for normal pooled fresh frozen plasma (FACT, George King Biomedicals) (black) and the same plasma incubated for 30 min with 100nM anti-fVIII antibodies (single-chain variable antibody fragment KM33 (7) (red) or 0.1 mg/ml anti-fXI antiboies (clone anti-FXI-2, Haematologic Technologies, Inc, (8) (blue) . The experiment was performed as described in the main text using 4μM of phospholipid vesicles and 800 μM of the fluorogenic substrate. Both antibodies inhibit clot growth in a similar manner showing that these two positive feedbacks play similar roles in the coagulation system.

Supporting Tables

Table S1. Thrombin reconstruction parameters

Description	Designation	Value
Spatial differentiation step	$i \cdot \Delta x$	258 μm
Temporal differentiation step	$j \cdot \Delta t$	120 s
Michaelis constant for the fluorogenic substrate	K_M	156 μM
Catalytic constant for the fluorogenic substrate	k_{cat}	0.8 s^{-1}
Width of the averaging region		430 μm
Free AMC diffusion coefficient	D_{AMC}	1,000 $\mu m^2 s^{-1}$
Bound AMC diffusion coefficient	D_{BSA}	50 $\mu m^2 s^{-1}$
Effect of clot on fluorescence	k_1	0.307 μM
Effect of clot on fluorescence	k_2	0.032 a.u.
Effect of clot on fluorescence	k_3	12,000 a.u.

Table S2. Model parameters: concentrations

Factor	Designation	Concentration (nM except for densities)	Factor	Designation	Concentration (nM except for densities)
1. Initial values of model variables[a]					
VIIa–TF	x_{7-3}^{S}	0			
VII–TF	y_{7-3}^{S}	0	VIIIa	x_8	0
TF	x_3^{S}	0.5 pmol/m^2	VIII	y_8	0.7
VIIa	x_7	0.1	Va	x_5	0
VII	y_7	10	V	y_5	20
IXa	x_9	0	XIa	x_{11}	0
IX	y_9	90	XI	y_{11}	30
Xa	x_{10}	0	ATIII	i_1	3,400
X	y_{10}	170	TFPI	i_2	2.5
IIa	x_2	0	Xa–TFPI	i_3	0
II	y_2	1,400	PCa	i_4	0
Fibrin	x_1	0	PC	i_5	60
Fibrinogen	y_1	7,600	Tm	i_{13}	special[b]
2. Constant concentrations[a]					
phospholipid	p	7.5·10-5[c]	heparin cofactor II	i_9	1,400
α_2-macroglobulin	i_6	1,500	protein C inhibitor	i_{10}	88
α_1-antitrypsin	i_7	40,000	C1 inhibitor	i_{11}	1,700
α_2-antiplasmin	i_8	1,100	protein S	i_{12}	346

[a] Concentrations are mostly from references (9, 10).

[b] Concentration or density is specified in figure legends for each numerical experiment.

[c] Procoagulant surface in platelet-free plasma as expressed in activated platelet equivalents (6).

Table S3. Model parameters: rate constants

Parameter	Value	Reference
	Clotting initiation:	
k_1, k_{-1}	4.2 $nM^{-1}min^{-1}$, 1.1 min^{-1}	(11, 12) [a]
k_2	0.0014 $nM^{-1}min^{-1}$	(13)
k_3	0.4 $nM^{-1}min^{-1}$	(14)
	Clotting cascade:	
k_4, K_4	630 min^{-1}, 210 nM	(15, 16)
k_5, K_5	5.8 min^{-1}, 200 nM	(17)
k_6, K_6	435 min^{-1}, 238 nM	(18)
k_7, K_7	0.06 min^{-1}, 230 molecules/platelet	(19, 20) [a]
k_8	6,350 min^{-1}	(21)
K_8	1,216 molecules/platelet	(21)
K_9	278 molecules/platelet	(21)
K_{10}	1,655 molecules/platelet	(21)
k_{11}, k_{-11}	0.052 $nM^{-1}min^{-1}$, 0.02 min^{-1}	(22)
k_{12}	45 $nM^{-2}min^{-1}$	(23, 24) [a]
k_{13}	1.44 min^{-1}	(25) [a]
k_{14}, K_{14}	5,040 min^{-1}, 7,200 nM	(26)
k_{15}, K_{15}	54 min^{-1}, 147 nM	(27)
k_{16}, K_{16}	14 min^{-1}, 71.7 nM	(28)
k_{17}	0.03 $nM^{-2}min^{-1}$	(29) [a]
k_{18}	0.0004 $min^{-1}nM^{-1}$	(30, 31) [a]
k_{-19}	770 min^{-1}	(32)
n_{20}, K_{20}	260 sites/platelet, 2.57 nM	(33)
n_{21}, K_{21}	750 sites/platelet, 1.5 nM	(34)
K_{22}	150 nM	(35)
K_{23}	0.118 nM	(23)
K_{24}	200 nM	(36) [a]

Parameter	Value	Reference
n_{25}, K_{25}, K_{26}	16,000 sites/platelet, 320 nM, 470 nM	(37)
n_{27}, K_{27}	2,700 sites/platelet, 2.9 nM	(23, 38)
	Inhibition:	
h_1	0.44 $nM^{-1}min^{-1}$	(22)
h_2	6 $nM^{-1}min^{-1}$	(32)
h_3	0.0000082 $nM^{-1}min^{-1}$	(39)
h_4	0.00015 $nM^{-1}min^{-1}$	(40)
h_5	0.00004 $nM^{-1}min^{-1}$	(41)
h_6	0.0000136 $nM^{-1}min^{-1}$	(41)
h_7	0.0012 $nM^{-1}min^{-1}$	(42)
h_8	0.000022 $nM^{-1}min^{-1}$	(43)
h_9	0.000336 $nM^{-1}min^{-1}$	(44)
h_{10}	0.0000293 $nM^{-1}min^{-1}$	(44)
h_{11}	0.00000651 $nM^{-1}min^{-1}$	(44)
h_{12}	0.00037 $nM^{-1}min^{-1}$	(42)
h_{13}	0.000063 $nM^{-1}min^{-1}$	(45)
h_{14}	0.35 min^{-1}	(46)
h_{15}	7.7 $nM^{-1}min^{-1}$	(47) [a]
h_{16}	0.000019 $nM^{-1}min^{-1}$	(48)
h_{17}	0.000026 $nM^{-1}min^{-1}$	(48)
h_{18}	0.000006 $nM^{-1}min^{-1}$	(48)
h_{19}	0.0054 $nM^{-1}min^{-1}$	(42)
h_{20}	0.00014 $nM^{-1}min^{-1}$	(49)
h_{21}	0.000006 $nM^{-1}min^{-1}$	(50)
h_{22}	0.000006 $nM^{-1}min^{-1}$	(50)
h_{23}	0.0000007 $nM^{-1}min^{-1}$	(51)
h_{24}	0.00039 $nM^{-1}min^{-1}$	(42)
	Substrate:	
$K_{S,2}$	150 μM	This study
$K_{S,10}$	878 μM	This study

Parameter	Value	Reference
	Phospholipids:	
K_p	50×10^{-5}nM	(52) [a]
	Thrombomodulin reactions:	
k_{28}, k_{-28}	0.4 $nM^{-1}min^{-1}$, 2 min^{-1}	(53)
k_{29}, K_{29}	370 min^{-1}, 7,600 nM	(54)
h_{25}	0.000312 $nM^{-1}min^{-1}$	(55)
h_{26}	0.14 $nM^{-1}min^{-1}$	(56)

[a] Estimation based on experimental data.

Supporting Movies

Movie S1. Temporally and spatially resolved imaging of clot growth and thrombin activity in blood plasma. This movie shows the formation and propagation of thrombin activity and a fibrin clot in plasma stimulated with immobilized TF (90 pmol/m^2). Imaging of thrombin activity in blood plasma from a healthy individual reveals a propagating wave. Upper row: The fibrin clot illuminated with red light grows from the activation surface (left). Thrombin formed during this process cleaves the substrate, and the fluorescence of released AMC is recorded (right). Lower row: Light scattering intensity (left) and distribution of thrombin concentration calculated from the AMC fluorescence intensity distribution (right).

Movie S2. Deceleration and cessation of thrombin wave in the presence of thrombomodulin. This movie demonstrates the deceleration and cessation of the thrombin wave in the presence of thrombomodulin (TF density is 4 pmol/m^2). Upper row: When the thrombomodulin concentration is high enough (1.5 nM), cessation of the thrombin wave can be observed. Light scattering intensity profile (left) and thrombin concentration profile (right) are shown. Clot growth rate decreases up to the full stop, and spreading of the thrombin wave stops. Lower row: In the case of a lower thrombomodulin concentration, the thrombin peak decelerates gradually, with a decrease in height (right). Light scattering profiles are shown on the left.

Supporting References

1. Hemker HC, Giesen PL, Ramjee M, Wagenvoord R, Beguin S (2000) The thrombogram: monitoring thrombin generation in platelet-rich plasma. Thromb Haemost **83:** 589-591.
2. Ovanesov MV, Ananyeva NM, Panteleev MA, Ataullakhanov FI, Saenko EL (2005) Initiation and propagation of coagulation from tissue factor-bearing cell monolayers to plasma: initiator cells do not regulate spatial growth rate. J Thromb Haemost **3:** 321-331.
3. Hemker HC & Beguin S (1995) Thrombin generation in plasma: its assessment via the endogenous thrombin potential. Thromb Haemost **74:** 134-138.
4. Hairer, E., Norsett, S. P., & Wanner, G. (1993) *Solving Ordinary Differential Equations 1: Nonstiff Problems*.
5. Panteleev MA, Balandina AN, Lipets EN, Ovanesov MV, Ataullakhanov FI (2010) Task-oriented modular decomposition of biological networks: trigger mechanism in blood coagulation. Biophys J **98:** 1751-1761.
6. Panteleev MA *et al.* (2006) Spatial propagation and localization of blood coagulation are regulated by intrinsic and protein C pathways, respectively. Biophys J **90:** 1489-1500.
7. Meems H, Meijer AB, Cullinan DB, Mertens K, Gilbert GE (2009) Factor VIII C1 domain residues Lys 2092 and Phe 2093 contribute to membrane binding and cofactor activity. Blood **114:** 3938-3946.
8. Butenas S *et al.* (2008) Factor XIa and tissue factor activity in patients with coronary artery disease. Thromb Haemost **99:** 142-149.
9. Butenas S & Mann KG (2002) Blood coagulation. Biochemistry (Mosc) **67:** 3-12.
10. Colman, R. W. (2006) *Hemostasis and thrombosis: basic principles and clinical practice* (Lippincott Williams & Wilkins, Philadelphia, PA).
11. Krishnaswamy S (1992) The interaction of human factor VIIa with tissue factor. J Biol Chem **267:** 23696-23706.

12. Nemerson Y & Gentry R (1986) An ordered addition, essential activation model of the tissue factor pathway of coagulation: evidence for a conformational cage. Biochemistry **25:** 4020-4033.

13. Butenas S & Mann KG (1996) Kinetics of human factor VII activation. Biochemistry **35:** 1904-1910.

14. Rao LV, Williams T, Rapaport SI (1996) Studies of the activation of factor VII bound to tissue factor. Blood **87:** 3738-3748.

15. Komiyama Y, Pedersen AH, Kisiel W (1990) Proteolytic activation of human factors IX and X by recombinant human factor VIIa: effects of calcium, phospholipids, and tissue factor. Biochemistry **29:** 9418-9425.

16. Warn-Cramer BJ & Bajaj SP (1986) Intrinsic versus extrinsic coagulation. Kinetic considerations. Biochem J **239:** 757-762.

17. Gailani D, Ho D, Sun MF, Cheng Q, Walsh PN (2001) Model for a factor IX activation complex on blood platelets: dimeric conformation of factor XIa is essential. Blood **97:** 3117-3122.

18. Baugh RJ & Krishnaswamy S (1996) Role of the activation peptide domain in human factor X activation by the extrinsic Xase complex. J Biol Chem **271:** 16126-16134.

19. Scandura JM & Walsh PN (1996) Factor X bound to the surface of activated human platelets is preferentially activated by platelet-bound factor IXa. Biochemistry **35:** 8903-8913.

20. Rawala-Sheikh R, Ahmad SS, Ashby B, Walsh PN (1990) Kinetics of coagulation factor X activation by platelet-bound factor IXa. Biochemistry **29:** 2606-2611.

21. Panteleev MA, Saenko EL, Ananyeva NM, Ataullakhanov FI (2004) Kinetics of factor X activation by the membrane-bound complex of factor IXa and factor VIIIa. Biochem J **381:** 779-794.

22. Baugh RJ, Broze GJ, Jr., Krishnaswamy S (1998) Regulation of extrinsic pathway factor Xa formation by tissue factor pathway inhibitor. J Biol Chem **273:** 4378-4386.

23. Tracy PB, Eide LL, Mann KG (1985) Human prothrombinase complex assembly and function on isolated peripheral blood cell populations. J Biol Chem **260:** 2119-2124.

24. van Dieijen G, Tans G, Rosing J, Hemker HC (1981) The role of phospholipid and factor VIIIa in the activation of bovine factor X. J Biol Chem **256:** 3433-3442.

25. Keuren JF *et al.* (2005) Synergistic effect of thrombin on collagen-induced platelet procoagulant activity is mediated through protease-activated receptor-1. Arterioscler Thromb Vasc Biol **25:** 1499-1505.

26. Higgins DL, Lewis SD, Shafer JA (1983) Steady state kinetic parameters for the thrombin-catalyzed conversion of human fibrinogen to fibrin. J Biol Chem **258:** 9276-9282.

27. Hill-Eubanks DC & Lollar P (1990) von Willebrand factor is a cofactor for thrombin-catalyzed cleavage of the factor VIII light chain. J Biol Chem **265:** 17854-17858.

28. Monkovic DD & Tracy PB (1990) Activation of human factor V by factor Xa and thrombin. Biochemistry **29:** 1118-1128.

29. Oliver JA, Monroe DM, Roberts HR, Hoffman M (1999) Thrombin activates factor XI on activated platelets in the absence of factor XII. Arterioscler Thromb Vasc Biol **19:** 170-177.

30. Yang L, Manithody C, Rezaie AR (2006) Activation of protein C by the thrombin-thrombomodulin complex: cooperative roles of Arg-35 of thrombin and Arg-67 of protein C. Proc Natl Acad Sci U S A **103:** 879-884.

31. Bush LA, Nelson RW, Di CE (2006) Murine thrombin lacks Na+ activation but retains high catalytic activity. J Biol Chem **281:** 7183-7188.

32. Panteleev MA, Zarnitsina VI, Ataullakhanov FI (2002) Tissue factor pathway inhibitor: a possible mechanism of action. Eur J Biochem **269:** 2016-2031.

33. Ahmad SS, Rawala-Sheikh R, Walsh PN (1989) Comparative interactions of factor IX and factor IXa with human platelets. J Biol Chem **264:** 3244-3251.

34. Ahmad SS, Scandura JM, Walsh PN (2000) Structural and functional characterization of platelet receptor-mediated factor VIII binding. J Biol Chem **275:** 13071-13081.

35. Koppelman SJ, Hackeng TM, Sixma JJ, Bouma BN (1995) Inhibition of the intrinsic factor X activating complex by protein S: evidence for a specific binding of protein S to factor VIII. Blood **86:** 1062-1071.

36. Hackeng TM, van ', V, Meijers JC, Bouma BN (1994) Human protein S inhibits prothrombinase complex activity on endothelial cells and platelets via direct interactions with factors Va and Xa. J Biol Chem **269:** 21051-21058.

37. Scandura JM, Ahmad SS, Walsh PN (1996) A binding site expressed on the surface of activated human platelets is shared by factor X and prothrombin. Biochemistry **35:** 8890-8902.

38. Tracy PB, Nesheim ME, Mann KG (1992) Platelet factor Xa receptor. Methods Enzymol **215:** 329-360.

39. Pieters J, Willems G, Hemker HC, Lindhout T (1988) Inhibition of factor IXa and factor Xa by antithrombin III/heparin during factor X activation. J Biol Chem **263:** 15313-15318.

40. Rezaie AR (1998) Calcium enhances heparin catalysis of the antithrombin-factor Xa reaction by a template mechanism. Evidence that calcium alleviates Gla domain antagonism of heparin binding to factor Xa. J Biol Chem **273:** 16824-16827.

41. Ellis V, Scully M, MacGregor I, Kakkar V (1982) Inhibition of human factor Xa by various plasma protease inhibitors. Biochim Biophys Acta **701:** 24-31.

42. Espana F, Berrettini M, Griffin JH (1989) Purification and characterization of plasma protein C inhibitor. Thromb Res **55:** 369-384.

43. Ellis V, Scully MF, Kakkar VV (1984) Inhibition of prothrombinase complex by plasma proteinase inhibitors. Biochemistry **23:** 5882-5887.

44. Downing MR, Bloom JW, Mann KG (1978) Comparison of the inhibition of thrombin by three plasma protease inhibitors. Biochemistry **17:** 2649-2653.

45. Derechin VM, Blinder MA, Tollefsen DM (1990) Substitution of arginine for Leu444 in the reactive site of heparin cofactor II enhances the rate of thrombin inhibition. J Biol Chem **265:** 5623-5628.

46. Lollar P, Parker ET, Fay PJ (1992) Coagulant properties of hybrid human/porcine factor VIII molecules. J Biol Chem **267:** 23652-23657.

47. Solymoss S, Tucker MM, Tracy PB (1988) Kinetics of inactivation of membrane-bound factor Va by activated protein C. Protein S modulates factor Xa protection. J Biol Chem **263:** 14884-14890.

48. Wuillemin WA *et al.* (1996) Modulation of contact system proteases by glycosaminoglycans. Selective enhancement of the inhibition of factor XIa. J Biol Chem **271:** 12913-12918.

49. Meijers JC, Vlooswijk RA, Bouma BN (1988) Inhibition of human blood coagulation factor XIa by C-1 inhibitor. Biochemistry **27:** 959-963.

50. Heeb MJ, Gruber A, Griffin JH (1991) Identification of divalent metal ion-dependent inhibition of activated protein C by alpha 2-macroglobulin and alpha 2-antiplasmin in blood and comparisons to inhibition of factor Xa, thrombin, and plasmin. J Biol Chem **266:** 17606-17612.

51. Heeb MJ, Bischoff R, Courtney M, Griffin JH (1990) Inhibition of activated protein C by recombinant alpha 1-antitrypsin variants with substitution of arginine or leucine for methionine358. J Biol Chem **265:** 2365-2369.

52. Panteleev MA, Ananyeva NM, Greco NJ, Ataullakhanov FI, Saenko EL (2006) Factor VIIIa regulates substrate delivery to the intrinsic factor X-activating complex. FEBS J **273:** 374-387.

53. Baerga-Ortiz A, Rezaie AR, Komives EA (2000) Electrostatic dependence of the thrombin-thrombomodulin interaction. J Mol Biol **296:** 651-658.

54. Galvin JB, Kurosawa S, Moore K, Esmon CT, Esmon NL (1987) Reconstitution of rabbit thrombomodulin into phospholipid vesicles. J Biol Chem **262:** 2199-2205.

55. Aritomi M *et al.* (1993) Recombinant human soluble thrombomodulin delivers bounded thrombin to antithrombin III: thrombomodulin associates with free thrombin and is recycled to activate protein c. Thromb Haemost **70:** 418-422.

56. Rezaie AR, Cooper ST, Church FC, Esmon CT (1995) Protein C inhibitor is a potent inhibitor of the thrombin-thrombomodulin complex. J Biol Chem **270:** 25336-25339.